NeuroImage: Clinical 12 (2016) 212–218

Contents lists available at ScienceDirect

NeuroImage: Clinical

journal homepage: www.elsevier.com/locate/ynicl

Giant early components of somatosensory evoked potentials to tibial nerve stimulation in cortical myoclonus

Francesca Anzellotti[a], Marco Onofrj[a,b], Laura Bonanni[a,b], Antonio Saracino[a], Raffaella Franciotti[b,c,*]

[a] Department of Neurology, SS Annunziata Hospital, Chieti, Italy
[b] Department of Neuroscience, Imaging and Clinical Sciences, "G. d'Annunzio" University and Aging Research Centre, Ce.S.I., "G. d'Annunzio" University Foundation, Chieti, Italy
[c] ITAB, "G. d'Annunzio" University Foundation, Chieti, Italy

ARTICLE INFO

Article history:
Received 29 September 2015
Received in revised form 24 June 2016
Accepted 1 July 2016
Available online 02 July 2016

Keywords:
Cortical myoclonus
Magnetoencephalography
Somatosensory evoked potential
Somatosensory evoked field
Motor cortex
Tibial nerve stimulation

ABSTRACT

Enlarged cortical components of somatosensory evoked potentials (giant SEPs) recorded by electroencephalography (EEG) and abnormal somatosensory evoked magnetic fields (SEFs) recorded by magnetoencephalography (MEG) are observed in the majority of patients with cortical myoclonus (CM). Studies on simultaneous recordings of SEPs and SEFs showed that generator mechanism of giant SEPs involves both primary sensory and motor cortices. However the generator sources of giant SEPs have not been fully understood as only one report describes clearly giant SEPs following lower limb stimulation. In our study we performed a combined EEG-MEG recording on responses elicited by electric median and tibial nerve stimulation in a patient who developed consequently to methyl bromide intoxication CM with giant SEPs to median and tibial nerve stimuli.
SEPs wave shapes were identified on the basis of polarity-latency components (e.g. P15-N20-P25) as defined by earlier studies and guidelines. At EEG recording, the SEP giant component did not appear in the latency range of the first cortical component for median nerve SEP (N20), but appeared instead in the range of the P37 tibial nerve SEP, which is currently identified as the first cortical component elicited by tibial nerve stimuli. Our MEG and EEG SEPs recordings also showed that components in the latency range of P37 were preceded by other cortical components. These findings suggest that lower limb P37 does not correspond to upper limb N20. MEG results confirmed that giant SEFs are the second component from both tibial (N43m-P43m) and median (N27m-P27m) nerve stimulation. MEG dipolar sources of these giant components were located in the primary sensory and motor area.

1. Introduction

Cortical myoclonus (CM) can be defined as involuntary brief muscle jerks originating from an abnormal discharge in the cerebral cortex: electroencephalographic (EEG) changes (positive spikes, spike and wave complexes or negative sharp waves) over the contralateral sensorimotor cortex are reported to precede CM (Obeso et al., 1985). By means of magnetoencephalography (MEG), Uesaka et al. (1996) identified 3 types of CM: cortical reflex myoclonus, sensorimotor cortical reflex myoclonus and motor cortical myoclonus. The first 2 types generate from the sensory cortex and result in both reflex and spontaneous myoclonus. Both were considered to be essentially stimulus-sensitive, and the spontaneous myoclonus probably results from unnoticed somatosensory inputs. Cortical reflex and sensorimotor cortical reflex myoclonus depend on abnormal enhancement of sensory and sensorimotor cortices excitability. The motor cortical myoclonus was thought to be primarily generated by spontaneous discharges in the motor cortex (Celesia et al., 1994; Uesaka et al., 1996). Postcentral cortex is considered the source of pre-myoclonus cerebral activity (Hitomi et al., 2006), despite earlier, challenging, reports (Mima et al., 1998).

Since the initial studies by Dawson (Dawson, 1946), which described somatosensory evoked potentials (SEPs) in humans, it is known that one of the main characteristics of the CM is the presence of very high-amplitude SEPs (giant SEPs) (Hallett et al., 1979; Rothwell et al., 1984; Shibasaki et al., 1978).

The majority of studies showed evidence of giant SEPs only to median nerve stimulation: these giant SEPs consisted of increased amplitude of the components appearing after the N20, which is thought to represent the first cortical postsynaptic activation corresponding to afference in primary idiotipic postrolandic cortex (Desmedt and Cheron, 1980; Desmedt et al., 1987; Mauguiére et al., 1983).

The giant SEPs to median nerve stimulation were characterized by normal amplitude of P14 and N20 and by appearance of high amplitude complexes in the latency range of P25-N30. The P25-N30 complex of normal SEPs is thought to represent activity of perirolandic cortex, possibly supplementary motor area (SMA) and associative somatosensory cortex, areas 2–3 (Desmedt and Cheron, 1980; Desmedt et al., 1987; Mauguiére et al., 1983). The giant SEPs in the latency range of P25-

* Corresponding author at: Department of Neuroscience, Imaging and Clinical Science, "G. d'Annunzio" University, Via dei Vestini 33, 66013 Chieti, Italy.
E-mail address: raffaella.franciotti@itab.unich.it (R. Franciotti).

http://dx.doi.org/10.1016/j.nicl.2016.07.001

N30 are thought to be dependent on the activation of new generators (Ikeda et al., 1995; Valeriani et al., 1997) or simply to an increase in the amplitude of the P25-N30 components of the normal response (Kakigi and Shibasaki, 1987a).

While there is agreement on the features (i.e. latency, topography) of giant SEPs to median nerve stimuli, there are only two studies showing that also SEPs to stimuli of lower limbs nerves might be giant (Hitomi et al., 2006; Kakigi and Shibasaki, 1987b). This is probably because the diseases inducing CM and giant SEPs appear with different involvement of peripheral nerves and CM to lower limb stimulation could be concealed by coexisting neuropathy (Fournier-Goodnight et al., 2015). In the present report we describe SEP and somatosensory evoked field (SEF) by means of MEG recordings, and their topography in a patient affected by CM of upper and lower limbs. The study allowed a comparison of the giant components of the upper and lower limbs and a discussion of possible generators.

A previous electrophysiological study from our Institution (Uncini et al., 1990) described a case of myoclonus after methyl bromide intoxication. The authors found that myoclonus, which was characterized by myoclonic jerks of the upper and lower limbs, belonged to the cortical reflex myoclonus type. In the patient presented in that report, CM persisted despite several pharmacological treatments attempts. Thus, we could record several years later, giant SEPs and SEFs following median and tibial nerve stimulation in the same patient.

2. Materials and methods

2.1. Patient and control group

Previously, we described (Uncini et al., 1990) a 13-year-old girl that had slept one night in a warehouse for wheat which had been sprayed a few hours before with methyl bromide as an insect fumigant. The morning after she woke up with headache, dizziness and nausea. At lunch time she was found unconscious in bed and was admitted to the intensive care unit where she developed generalized seizures. After 3 days her level of consciousness gradually improved and myoclonic jerks, at times generalized, appeared. The patient was initially unsuccessfully treated with phenobarbital 250 mg/day and acute i.v. administration of phenytoin (1000 mg). No reduction of frequency and intensity of myoclonic jerks was noted. Four weeks later, the patient, who was at the time oriented and cooperative, was transferred to our department. We ineffectively attempted to treat the patient with sodium valproate (up to 60 mg/Kg) and L-5-hydroxytryptophan (800 mg/day) with carbidopa (100 mg/day) or chlorimipramine (50 mg/day) were also unsuccessfully administered to the patient. During her two-month stay in our department we observed periodic gradual increase of myoclonic jerks culminating on at least 2 occasions in a grand mal attack.

We had the chance to observe the same patient 20 years later: at rest, frequent myoclonic jerks of the limbs were present and myoclonus was also induced by somatosensory stimuli as touching or tendon tapping. Any attempt of voluntary limb movements or passive displacement of limbs provoked a series of jerks and often gave rise to generalized jerks involving the entire body. Myoclonic jerks disappeared only when the patient was sleeping or floating in a swimming pool. Gait was wide-based, continuously hampered by myoclonus and impossible without assistance. Speech was dysarthric. Muscle tone was normal. Plantar responses were in flexion. There were no sensory abnormalities. Cerebral CT and MRI were normal. Through time, several attempts were made to reduce myoclonus, by introducing Clonazepam, Clobazam, Piracetam, Levetiracetam, Lamotrigine, Carbamazepine, Etosuccimide, Topiramate, Felbamate, Perampanel, Amantidine, Memantine, Gammahydroxybutirate, all attempts to treatment were unsuccessful. When SEPs and SEFs were recorded, her treatment consisted of 6 mg/day of clonazepam, 4000 mg/day of levetiracetam and 100 mg/day of Phenobarbital, as attempts to reduce these treatments resulted in increased frequency of generalized seizures.

SEP and MEG recordings were separately performed on the patient following left and right median and tibial nerve stimulations.

A control group consisting of 10 female healthy subjects (mean age 35 ± 4 years, ranging from 29 to 41 years) and mean height of 165 ± 5 cm) was selected from our neurophysiology laboratory. SEPs were recorded on the control group following left and right median and tibial nerve stimulations for comparison with the patient. The patient and all the control subjects signed a written informed consent to the study. The investigation was carried out according to the Declaration of Helsinki and subsequent revisions (Declaration of Helsinki, 1997).

2.2. Stimulation and recording

Somatosensory electrical stimuli were rectangular pulses with a repetition rate of 0.3 Hz. Stimuli were unilaterally delivered to right or left median nerve at the wrist or to the left and right tibial nerve at the medial malleolus. Intensities of stimulation were settled at a level producing a painless, clearly visible thumb opposition or foot flexion. The duration of the stimuli was set at 200 μs for the upper limbs and at 800 μs for the lower limbs. Stimuli were delivered by means of a pair of nonmagnetic, 3-cm-spaced, Ag-AgCl disk electrodes filled with conductive gel, via a twisted and shielded pair of wires for MEG recordings.

SEPs after median and tibial nerve stimulation were recorded with Ag/AgCl disk electrodes placed on 19 derivations corresponding to the International 10–20 system. Reference was at the linked earlobes (A1 + A2). 130 artifact-free responses were separately recorded for each of the four stimulation sessions. Then, responses were averaged in a period of 100 ms from the onset of the stimuli to obtain SEPs for each recording session. The amplitude of each SEPs was calculated with respect to the amplitude at the onset of the stimuli.

EEG and MEG were recorded in separate session. During MEG recording, the patient was seated inside a magnetically shielded room. SEFs were recorded at 1025 Hz sampling rate using the whole-head MEG system consisting of 165 dc SQUID integrated magnetometers (Della Penna et al., 2000).

Before and after each stimulation session, the position of the head with respect to the sensor was determined by localizing five coils placed on subject's head. The locations of the coils and of three anatomical landmarks on the subject's head were digitized by means of a 3D digitizer (Polhemus, 3Space Fastrak).

A high-resolution structural volume was acquired with a Philips scanner at 3 T via a 3-D T1-TFE (Turbo Field Echo) sequence to provide the anatomical reference for the MEG recordings.

For each of the four stimulation sessions (left and right median nerve stimulation, left and right tibial nerve stimulation) MEG data were preprocessed to subtract the heart signal and to remove noisy trials. Thus the first artifact-free 130 responses were averaged in a period of 150 ms, including a 50 ms prestimulus time. The amplitude of SEFs was calculated with respect to a baseline level chosen as the mean value of the 10–15 ms post-stimulus baseline (Torquati et al., 2002). The SEFs were analyzed in the interval 18–120 ms post-stimulus. Data analysis was performed using the equivalent current dipole (ECD) as source model of the SEFs. Only dipolar source configurations with explained variance >90% were accepted. Source waveforms were estimated by multiple source analysis using the BESA-BrainVoyager software in the 0–100 time interval. For each dipolar source the greatest intensity and the latency of peak activity were estimated in order to compare the strength among sources. Then the intensity of the sources was normalized with respect to the source intensity of the first component. ECDs were superimposed on structural MRI images transformed into the Talairach space using a piecewise affine and continuous transformation to evaluate the location of the sources.

3. Results

3.1. SEPs following stimulation of the median nerve

Three components of SEPs following left and right median nerve stimulation were clearly identified at about 20 ms, 25 ms and 33 ms after the onset of the stimuli for both the patient and the control group.

Frontal P20, N25 and P33 and central N20, P25 and N33 components following left and right median nerve stimulation are shown in Fig. 1a for the patient (blue line) and for a representative subject of the control group (red line). Fig. 1b shows the flux maps of the patient and of the representative subject for the three components. Despite amplitude differences, the three components appear with same isofield scalp distributions in the patient and in the control subject. The first component has a negative peak in anterior derivation contralateral to the stimulation side and positive electric potential in posterior derivation. The second component has positive and negative electric potential in antero-posterior direction. The third component is distributed widely and has negative and positive electric potential in antero-posterior direction, as described in previous studies (Desmedt and Cheron, 1980; Desmedt et al., 1987; Mauguiére et al., 1983).

The peak latencies and amplitudes of the three components of SEPs at the frontal and central channels contralateral to the stimulation side are shown in Table 1 for the patient and the control group. Table 1 shows also cut off range expressed as normal mean minus and plus 3 SD.

The amplitudes and latencies of the first component of the cortical SEPs at frontal and central channel were similar for the patient and the control group for the left and the right median nerve stimulation. For the patient the amplitude of the P25 (central channel) and N25 (frontal channel) second components was outside the cut off range. It was increased by ten and five times as compared to the amplitude of the control group for central and frontal channel respectively. The second giant component of SEPs recorded in the patient was evident from both the left and the right median nerve stimulation. The peak latency of the second component did not differ between the patient and the control group. The amplitude of the third component was higher in the patient as compared to the control group, but the increase was lower than that of the second component. The amplitude of the N33 at the central channel was increased by three times, whereas the amplitude of the P33 at the frontal channel was increased by five times in the patient as compared to control group. The latency of the third component did not differ between the patient and the control group.

3.2. SEPs following stimulation of the posterior tibial nerve

Three components of SEPs following left and right tibial nerve stimulation were clearly identified at about 30 ms, 37 ms and 45 ms after the onset of the stimuli for both the patient and the control group.

SEPs at the fronto-central channel following the left and right tibial nerve stimulation are shown in Fig. 2a for the patient (blue line) and for a representative control subject (red line). Fig. 2b shows the flux maps of the patient and of the representative subject for the three

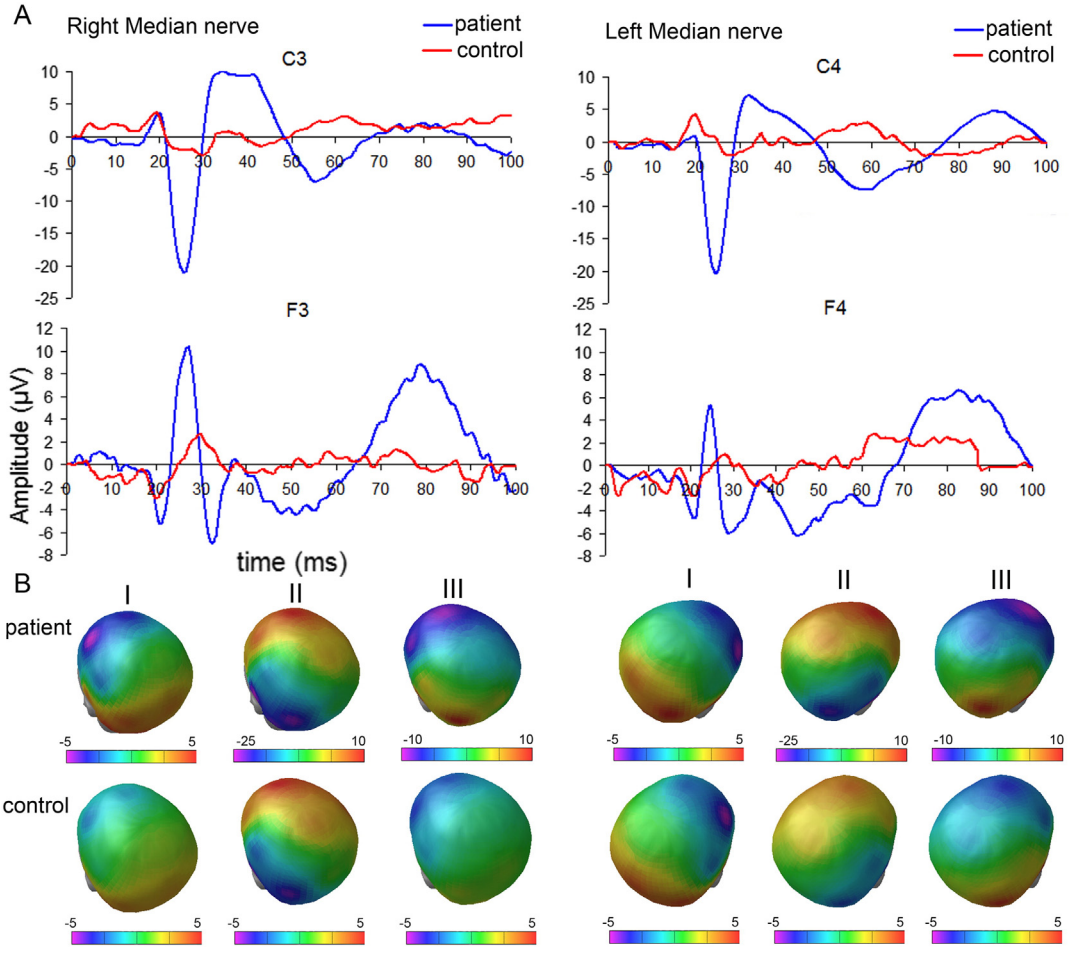

Fig. 1. Median nerve SEP a) Mean SEPs for the patient (blue line) and for a representative subject of the control group (red line). SEPs from the central (C3, C4) and frontal (F3, F4) electrode following the right and left median nerve stimulation respectively are shown. b) Flux map of the patient and a representative control subject for the three components at 20 ms, 25 ms and 33 ms from the stimulus onset. (For interpretation of the references to color in this figure legend, the reader is referred to the web version of this article.)

Table 1
Peak latencies and amplitudes of the three components of SEPs following median and tibial nerve stimulation for the patient and the control group. For control group values show mean ± SD and cut off range expressed as normal mean minus and plus 3 SD.

			Latency (ms)		Amplitude (μV)	
			Patient	Control group	Patient	Control group
			First component			
Left median nerve	C4	N20	19.5	20.0 ± 1.0 [17.0–23.1]	0.8	3.2 ± 1.1 [−0.2–6.5]
	F4	P20	21	21.0 ± 1.3 [17.0–25.0]	−4.7	−1.9 ± 1.2 [−5.5–1,6]
Right median nerve	C3	N20	20	20.0 ± 1.8 [14.5–25.5]	3.6	2.8 ± 0.7 [0.9–4.8]
	F3	P20	21	20.5 ± 1.9 [14.7–26.3]	−5.3	−1.9 ± 1.2 [−5.4–1.5]
Left tibial nerve	Cz-Fpz	N30	30	29.0 ± 7.8 [5.5–52.5]	1.7	0.8 ± 0.5 [−0.6–2.3]
Right tibial nerve	Cz-Fpz	N30	30	30.0 ± 5.6 [13.3–46.7]	1.8	1.2 ± 0.5 [−0.1–2.6]
Second component						
Left median nerve	C4	P25	25	24.0 ± 2.6 [16.1–31.9]	**−20.3**	−2.1 ± 1.1 [−5.3–1.0]
	F4	N25	25	27.5 ± 1.1 [24.1–30.8]	**5.3**	0.9 ± 0.6 [−0.8–2.7]
Right median nerve	C3	P25	26	25.0 ± 2.4 [17.7–32.4]	**−21**	−2.3 ± 1.2 [−6.0–1.3]
	F3	N25	27	28.0 ± 1.6 [23.1–32.9]	**10.4**	2.1 ± 1.2 [−1.4–5.6]
Left tibial nerve	Cz-Fpz	P37	**44**	35.5 ± 1.3 [31.5–39.5]	**−10.7**	−1.5 ± 0.6 [−3.2–0.2]
Right tibial nerve	Cz-Fpz	P37	**42.5**	36.0 ± 1.2 [32.5–39.5]	**−4.4**	−1.3 ± 0.5 [−2.8–0.2]
Third component						
Left median nerve	C4	N33	32	35.0 ± 3.8 [23.6–46.4]	**7.1**	2.2 ± 0.8 [−0.2–4.5]
	F4	P33	29	35.0 ± 3.2 [25.3–44.7]	**−6**	−1.2 ± 0.6 [−3.1–0.7]
Right median nerve	C3	N33	34.5	33.5 ± 5.6 [16.6–50.4]	**10.5**	3.4 ± 1.2 [−0.1–6.9]
	F3	P33	32.5	35.0 ± 2.7 [26.9–43.1]	**−7**	−1.4 ± 0.7 [−3.4–0.6]
Left tibial nerve	Cz-Fpz	N45	50	47.0 ± 2.4 [39.9–54.1]	**5.4**	1.2 ± 0.5 [−0.4–2.8]
Right tibial nerve	Cz-Fpz	N45	48	48.0 ± 1.5 [43.5–52.5]	**2.2**	1.5 ± 0.2 [0.9–2.1]

In the patient the abnormal values which are outside the cut off range shown in parenthesis are highlighted in bold.

components. As evident in Fig. 2b, despite the amplitude difference the isofield scalp distribution in the patient corresponds to scalp distribution in the control subject. The three components showed the typical scalp electric potential described by previous reports (Desmedt and Cheron, 1980; Desmedt et al., 1987; Mauguiére et al., 1983). The first component had the positive peak in the central area. The second component had negative electric potential widely distributed in the central area. The third component had a positive electric potential widely distributed in the central area.

The peak latencies and amplitudes of the three components of SEPs at the fronto-central channel for the patient and the control group are shown in Table 1.

The latencies and amplitude of the first component of the cortical SEPs was similar in the patient and the control group. In the patient the amplitude of the second component at fronto-central channel was increased and was outside the cut off range. The second component of the patient was three times and seven times the amplitude of the control group for the right and the left tibial nerve stimulation respectively.

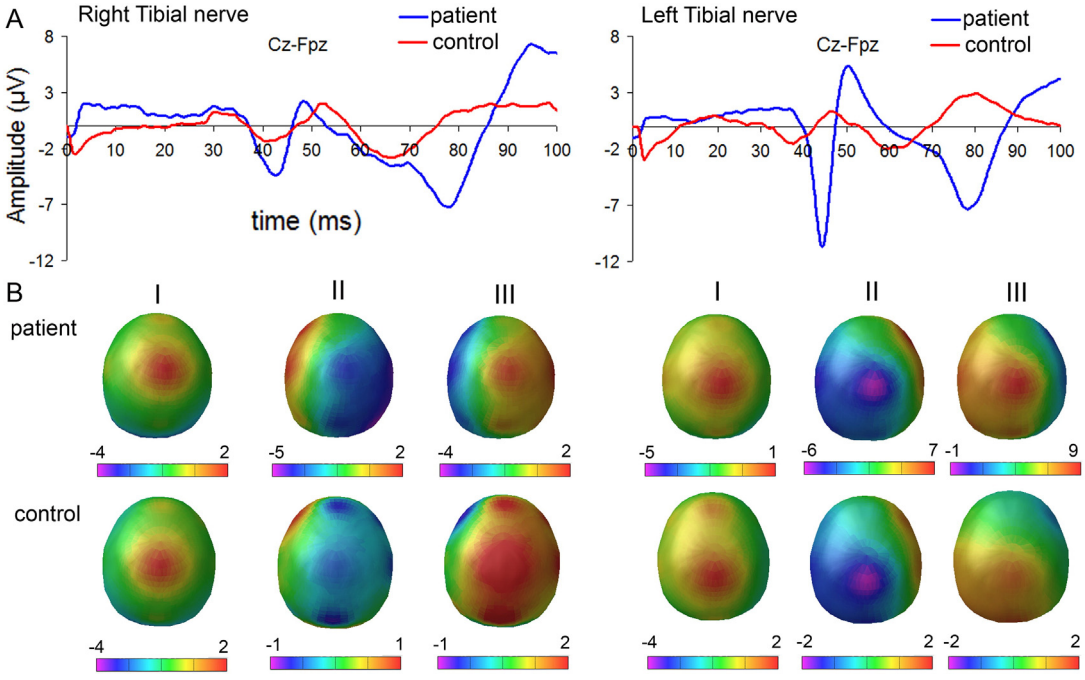

Fig. 2. Tibial nerve SEP a) Mean SEPs for the patient (blue line) and for a representative subject of the control group (red line). SEPs from the centro-frontal channel are shown. b) Flux map of the patient and a representative control subject for the three components at 30 ms, 37 ms and 45 ms from the stimulus onset. (For interpretation of the references to color in this figure legend, the reader is referred to the web version of this article.)

The peak latencies of the second component were also increased by 6 ms and 9 ms for the right and left limb respectively.

The amplitude of the third component at fronto-central channel was also outside the cut off range. It was slightly increased for the right side but it was increased by about four time for the left side. The latency of the third component was similar in the patient and control group.

3.3. SEFs following stimulation of the median nerve

Mean evoked magnetic fields of the patient following left and right median nerve stimulations showed four components: N22m-P22m, N27m-P27m, N33m-P33m, and N45m-P45m. For each of the four magnetic components, the intensity and locations of the ECD were estimated considering fit intervals ranging from 20 to 24 ms, from 25 to 29 ms, from 30 to 34 ms and from 42 to 48 ms, respectively. Fig. 3a shows the SEFs in two magnetic sensors for left and right median nerve stimulation. The amplitude of the N27m-P27m component was enlarged in the comparison with the other components (Fig. 3a). MEG field topography (Fig. 3b) shows the typical dipolar pattern for each of the four components.

Table 2 shows peak latencies and intensities of the dipolar sources of SEFs following median nerve stimulation and the normalized amplitudes with respect to the source intensity of the first component. The intensity of the dipolar source of N27m-P27m complex (second component) was greater than two times the intensity of the sources of the first component (Table 2).

Location and orientation of the dipolar sources in the standardized space of Talairach are shown in Table 3. All the four dipolar sources were located in the contralateral primary somatosensory and motor cortices (BA3 and 4).

3.4. SEFs following stimulation of the tibial nerve

Mean evoked magnetic fields of the patient following left and right tibial nerve stimulations showed six components: N34m-P34m, N43m-P43m, N46m-P46m, N50m-P50m, N67m-P67m, N79m-P79m. For each of the six magnetic components, the intensity and locations of the ECD were estimated considering fit intervals ranging from 32 to 36 ms, from 41 to 44 ms, from 45 to 47 ms, from 49 to 52 ms, from 65 to 69 ms, and from 75 to 84 ms, respectively. Fig. 3c shows the SEFs in four magnetic sensors for left and right tibial nerve stimulation. The amplitude of the N43m-P43m and the N79m-P79m complexes were enlarged as compared to the other components (Fig. 3c). MEG field topography (Fig. 3d) shows the typical dipolar pattern for each of the six components.

Table 2 shows peak latencies and intensities of the dipolar sources of SEFs following tibial nerve stimulation and the normalized amplitudes with respect to the source intensity of the first component. The intensity of the sources at 43 ms (second component) was greater than about six times and five times the intensity of the sources of the first component for the left and the right side respectively (Table 2). The intensity of the sources at 79 ms was seven times the intensity of the sources at 34 ms

Table 2
Peak latencies and intensities of the dipolar sources of SEFs following median and tibial nerve stimulation. Normalized amplitudes with respect to the source intensity of the first component are shown in parenthesis.

Latency (ms)	Dipole strength (nAm)		Latency (ms)	Dipole strength (nAm)
Median nerve stimulation				
LEFT 22	15 [1.0]	RIGHT	22	25 [1.0]
27	38 [2.5]		27	57 [2.3]
33	22 [1.5]		33	24 [1.0]
45	16 [1.1]		45	26 [1.0]
Tibial nerve stimulation				
LEFT 34	5 [1.0]	RIGHT	34	5 [1.0]
43	29 [5.8]		43	23 [4.6]
46	18 [3.6]		46	5 [1.0]
50	10 [2.0]		50	20 [4.0]
67	28 [5.6]		67	29 [5.8]
79	34 [6.8]		79	35 [7.0]

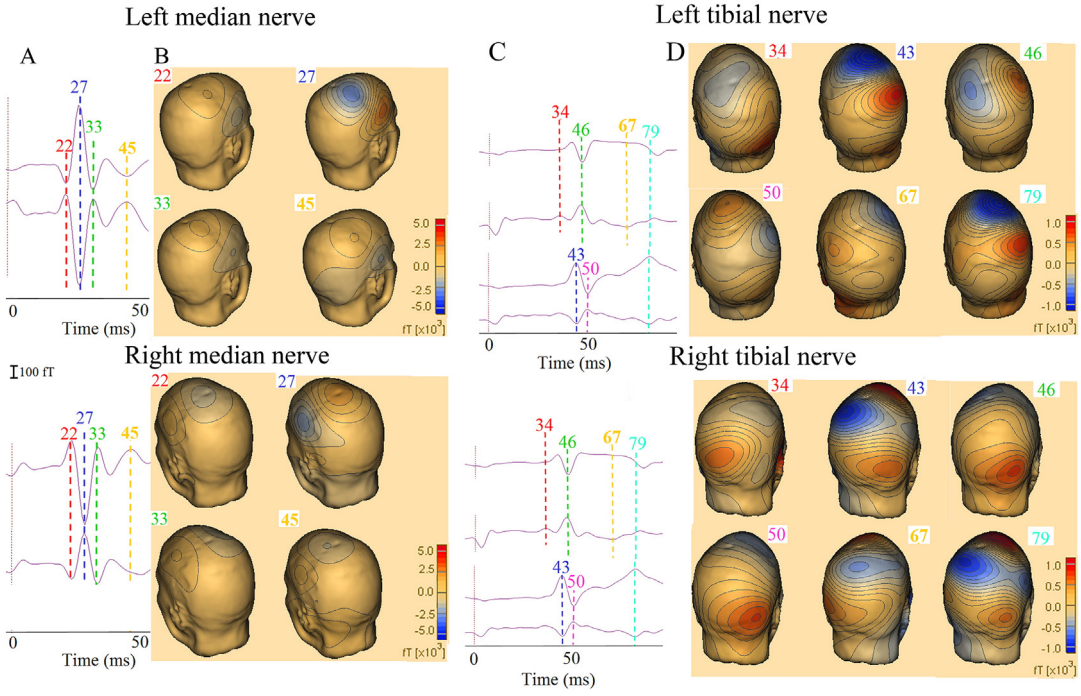

Fig. 3. Median and tibial nerve SEF a) Mean SEFs from two magnetic channels following the left and right median nerve stimulation showing four components: N22m-P22m (red line), N27m-P27m (blue line), N33m-P33m (green line), and N45m-P45m (yellow line). b) MEG field topography on patient structural MRI at 22 ms, 27 ms, 33 ms and 45 ms. c) Mean SEFs from four magnetic channels following the left and right tibial nerve stimulation showing six components: N34m-P34m (red line), N43m-P43m (blue line), N46m-P46m (green line), N50m-P50m (pink line), N67m-P67m (yellow line), N79m-P79m (cyan line). d) MEG field topography on patient structural MRI at 34 ms, 43 ms, 46 ms, 50 ms, 67 ms and 79 ms. (For interpretation of the references to color in this figure legend, the reader is referred to the web version of this article.)

Table 3
Location (X, Y, Z) and orientation (X-ori Y-ori Z-ori) of the dipolar MEG sources in the standardized space of Tailarach.

Peak (ms)	X Y Z (mm)	X-ori Y-ori Z-ori	BA		Peak (ms)	X Y Z (mm)	X-ori Y-ori Z-ori	BA
Median nerve stimulation								
L 22	47 −43 43	0.1 1.0 0.2	3	R	22	−43 −15 50	0.3 0.9 0.3	4
27	35 −38 48	0.1 0.9 0.3	3		27	−33 −23 55	0.1 1.0 0.1	4
33	37 −41 44	0.2 1.0 0.2	3		33	−28 −25 52	0.2 1.0 0.2	3
45	28 −33 51	0.2 1.0 0.2	3		45	−36 −27 51	0.0 1.0 0.1	3
Tibial nerve stimulation								
L 34	11 −50 55	−0.7 −0.7 −0.1	3	R	34	−5 −33 57	−1.0 0.0 −0.1	3
43	12 −27 57	−1.0 −0.0 0.2	4		43	−5 −24 58	0.8 −0.6 0.0	4
46	7 −36 56	−0.2 −1.0 −0.2	3		46	−5 −13 58	−0.3 −1.0 0.0	8
50	11 −30 57	0.9 0.4 −0.1	4		50	−1 −26 58	−1.0 0.0 0.0	4
67	3 −24 57	−0.4 0.9 0.1	4		67	−15 −12 53	0.1 1.0 0.0	8
79	15 −25 57	−0.9 0.3 0.3	4		79	−2 −25 56	1.0 0.2 0.1	4

BA: Brodmann area; L: left; R: right.

(Table 2). Location and orientation of the dipolar sources in the standardized space of Talairach are shown in Table 3. The first two components were located in the contralateral primary somatosensory-motor cortex (BA 3,4), whereas the last components were located more anteriorly in the frontal and central region (BA 4, 8).

4. Discussion

In our study we could record giant SEP to median and tibial nerve stimulation in a patient affected by CM, and compare latencies and topography of the evoked components with those registered in an age-matched control group. Whereas giant SEPs to median nerve stimuli are unequivocally defined, as regards to latency, topography and possible matches with normal SEPs components, the consistency of giant SEPs to tibial nerve stimuli is less known, as only two, non-topographical studies (Hitomi et al., 2006; Kakigi and Shibasaki, 1987b), showed enlarged SEP components. In those reports, giant SEPs to tibial nerve stimuli were recorded in one and three patients respectively. The latency of the giant SEPs was in both cases around 50 ms. This giant component to tibial nerve stimuli was, in both studies, identified as the first component appearing on scalp derivations, even though close inspection of recordings shown by one of the study (Kakigi and Shibasaki, 1987b) suggests that an earlier negative deflection was present.

In our study the giant SEPs components recorded in the CM patient was not the first scalp recorded component but the second, to median and tibial nerve stimuli, and this enlarged component was followed by another component of amplitude higher than the amplitude of the correspondent components recorded in the controls.

In patient and healthy subjects N20-P20, P25-N25 and N33-P33 responses were well identifiable in the centro-parietal and in the frontal region contralateral to the median nerve stimulation. The comparison between patient and control group evidenced that the second SEPs component P25-N25 was giant in the patient, confirming previous studies (Broughton et al., 1981; Goff et al., 1977; Lueders et al., 1983), while the early N20-P20 was of normal amplitude. Our study showed that the giant SEPs to tibial nerve stimuli were in the latency range of P37-N45, yet this component followed an earlier component of normal amplitude with a latency of 30 ms.

In response to median nerve stimuli also N33-P33 was of higher amplitude in the patient than in controls. In response to tibial nerve stimuli the giant P37 was also followed by a giant N45-P45.

MEG recordings of response to median and tibial nerve stimuli confirmed that the first elicited component was of normal amplitude while increased amplitudes were only found in the second and subsequent magnetic components (Fig. 3). SEFs recorded by MEG consisted of 4 components in response to median nerve stimuli and 6 components in response to tibial nerve stimuli.

SEPs and SEFs were not precisely matched in latency, as expected, because MEG is insensitive to radially oriented sources while SEP components are supposedly, generated, in part, by radially oriented sources (Baumgärtner et al., 2010). The discrepancy does not reduce the significance of our main finding, showing that, in CM, SEPs become giant only after the first cortical potential.

Therefore, at difference with SEPs, SEFs to median and tibial nerve stimuli consisted of a complex of 2 or 3 giant components following the first source component, which was characterized by normal amplitude.

We are well aware that a study in a single patient cannot be used to drive solid conclusions on location of generators of the giant signal, yet we believe that at least an hypothesis and a single conclusion could be presented to discussion.

The giant dipoles were only slightly anterior to the dipole corresponding to the first cortical afference despite the different latencies (Fig. 3). We suggest that the amplitude of giant SEFs could be dependent of the appearance of paroxysmal depolarization shifts in neurons receiving secondary afference from the first cortical somatosensory afference.

Our hypothesis suggests that the giant SEFs might be generated by both the source of normal SEPs components and different sources, due to repetitive depolarization in the same neural soma. Alternatively, our hypothesis suggests that the normal N20 to median nerve and normal N30 to tibial nerve is followed by a giant P25-N30 to median nerve, and a giant P37-N67-P79 to tibial nerve. The first giant component might be due to the increased amplitude of the same source generating normal components, but the complex of giant potential following the first giant signal might be due to different sources than normal SEPs, probably a recurrent source in the same area. Therefore our hypothesis could be considered an intermediate position between hypothesis of authors who believed that giant potentials are due to increased amplitude of normal signals (Kakigi and Shibasaki, 1987a) and authors who believe that giant potential are due to novel high voltage signals (Ikeda et al., 1995; Valeriani et al., 1997).

Unfortunately definitive conclusions on the position and orientation of the dipolar sources which generate these magnetic components cannot be drawn because larger sample of patients are required, and this is difficult due to the rarity of giant SEP to tibial nerve stimuli.

Our conclusion is dependent on the finding that giant SEPs following median nerve stimuli appear only after N20-P20 complex and the topography of this giant SEPs suggests that these giant components could be corresponding to P25-N30. For SEPs following lower limb stimuli, the giant components are instead corresponding to the P37 complex. As observed in our patient and controls the early lower limb component corresponding to upper limb N20 could be the N30 component (Table 1, Figs. 1,2). This finding suggests that, albeit probably useful for clinical purposes, the calculation of central conduction times, as currently adopted, should be reformulated on shorter latencies.

Cortical generators of SEPs following median nerve stimulation have been studied extensively (Deiber et al., 1986; Desmedt and Cheron,

1981; Desmedt et al., 1987; Lueders et al., 1983; Mauguiére et al., 1983) and a general agreement has been reached on the hypothesis that these components originated from area 3b (BA3b). The cortical origin of the P25-N25 is still debated (Allison et al., 1989; Desmedt et al., 1987): previous studies showed that the central N20-P25 and frontal P20-N25 complexes most likely represent a tangential dipole across the central fissure and most likely arise from posterior bank of the central fissure, area 3b (Desmedt et al., 1987). SEF studies on median nerve stimulation supported SEP findings, showing that central N20-P25 and frontal P20-N25 complexes corresponded to tangentially oriented current sources at the primary somatosensory cortex (Hari et al., 1984; Uesaka et al., 1996). An additional current source most likely representing partially peri-rolandic components was also suggested (Baumgartner et al., 1991). The first cortical SEF component, N20m, reversed polarity between the upper and lower ends of the central sulcus confirming previous reports (Hari et al., 1984; Huttunen et al., 1987; Kaukoranta et al., 1986; Rossini et al., 1987) and can also be explained by a tangential source in BA3b. The magnetic deflection around 30 ms, was considered to be generated by a tangential source in the posterior wall of the rolandic fissure medial to the generation site of N20m, and possibly in part in the motor cortex (Huttunen et al., 1987).

Fewer hypotheses on the generators of SEPs to tibial nerve stimuli were formulated: the conventional representation of dipole sources suggests that P37 is the equivalent of N20. We believe that our study shows that P37 is not the equivalent of N20, as a component in the range of P37 becomes giant in CM, and this is not the case for N20.

The effect of anticonvulsants and epileptic activity on our results should be discussed: probably the increase in the amplitude of some components might be related to a decreased activation of complex inhibitory mechanisms mediated by γ-aminobutyric acid (GABAergic) connections within the parietal cortex. Previous studies showed that antiepileptic drugs seem to either decrease or increase the amplitude of giant component of SEPs or SEFs, partly depending on the dosage (Ebner and Deuschl, 1988; Rothwell et al., 1984). More recently, SEP studies on the potential antiepileptic drugs-induced abnormalities showed no effect on nerve conduction and on the somatosensory tracts (Sendrowski et al., 2010) or a reduction of the amplitude of SEPs (Striano et al., 2005). Thus it remains to be solved what kind of effects those drugs have on electrophysiological analysis.

Finally age effect on SEP parameters should be also considered. The effects of age on SEP latencies mainly reflect conduction slowing in the peripheral nerves. Most of this change occurs after the age of 55 years (Allison et al., 1983). The amplitude of median nerve SEPs recorded in the frontal region tends to decrease with age while that of the parietal N20 tends to increase (Desmedt and Cheron, 1980). Age of our control group ranged from 29 to 41 years, thus recorded SEPs were not influenced by age effect.

References

Allison, T., McCarthy, G., Wood, C.C., Darcey, T.M., Spencer, D.S., Williamson, P.D., 1989. Human cortical potentials evoked by stimulation of the median nerve. I. Cytoarchitectonic areas generating short-latency activity. J. Neurophysiol. 62, 694–710.

Allison, T., Wood, C.C., Goff, W.R., 1983. Brainstem auditory, pattern-reversal visual and short-latency somatosensory evoked potentials: latencies in relation to age, sex, and brain and body size. Electroencephalogr. Clin. Neurophysiol. 55, 619–636.

Baumgartner, C., Barth, D.S., Levesque, M.F., Sutherling, W.W., 1991. Functional anatomy of human hand sensorimotor cortex fromspatiotemporal analysis of electrocorticography. Electroencephalogr. Clin. Neurophysiol. 78, 56–65.

Baumgärtner, U., Vogel, H., Ohara, S., Treede, R.D., Lenz, F.A., 2010. Dipole source analyses of early median nerve SEP components obtained from subdural grid recordings. J. Neurophysiol. 104, 3029–3041.

Broughton, R., Rasmussen, T., Branch, C., 1981. Scalp and direct cortical recordings of somatosensory evoked potentials in man (circa 1967). Can. J. Psychol. 35, 136–158.

Celesia, G.G., Parmeggiani, L., Brigell, M., 1994. Dipole source localization in a case of epilepsia partialis continua without premyoclonic EEG spikes. Electroencephalogr. Clin. Neurophysiol. 90, 316–319.

Dawson, G.D., 1946. The relation between the electroencephalogram and muscle action potentials in certain convulsive states. J. Neurol. Neurosurg. Psychiatry 9, 5–22.

Declaration of Helsinki, 1997. Recommendation guiding physicians in biomedical research involving human subjects. JAMA 277, 925–956.

Deiber, M.P., Giard, M.H., Mauguiére, F., 1986. Separate generators with distinct orientations for N20 and P22 somatosensory evoked potentials to finger stimulation? Electroencephalogr. Clin. Neurophysiol. 65, 321–334.

Della Penna, S., Del Gratta, C., Granata, C., Pasquarelli, A., Pizzella, V., Rossi, R., Russo, M., Torquati, K., Erné, S.N., 2000. Biomagnetic systems for clinical use. Philos. Mag. B 80, 937–948.

Desmedt, E., Cheron, G., 1980. Somatosensory evoked potentials to finger stimulation in healthy octogenarians and in young adults: wave forms, scalp topography and transit times of parietal and frontal components. Electroencephalogr. Clin. Neurophysiol. l50, 404–425.

Desmedt, J.E., Nguyen, T.H., Bourguet, M., 1987. Bit-mapped color imaging of human evoked potentials with reference to the N20, P22, P27 and N30 somatosensory responses. Electroencephalogr. Clin. Neurophysiol. 68, 1–19.

Ebner, A., Deuschl, G., 1988. Frontal and parietal components of enhanced somatosensory evoked potentials: a comparison between pathological and pharmacologically induced conditions. Electroencephalogr. Clin. Neurophysiol. 71, 170–179.

Fournier-Goodnight, A.S., Gabriel, M., Perry, M.S., 2015. Preliminary neurocognitive outcomes in Jeavons syndrome. Epilepsy Behav. 52, 260–263.

Goff, G.D., Matsumiya, Y., Allison, T., Goff, W.R., 1977. The scalp topography of human somatosensory and auditory evoked potentials. Electroencephalogr. Clin. Neurophysiol. 42, 57–76.

Hallett, M., Chadwick, D., Marsden, C.D., 1979. Cortical reflex myoclonus. Neurology 29, 1107–1125.

Hari, R., Renikainen, K., Kaukoranta, E., Hämäläinen, M., Ilmoniemi, R., Penttinen, A., Salminen, J., Teszner, P., 1984. Somatosensory evoked cerebral magnetic fields from SI and SII in man. Electroencephalogr. Clin. Neurophysiol. 57, 254–263.

Hitomi, T., Ikeda, A., Matsumoto, R., Kinoshita, M., Taki, J., Usui, K., Mikuni, N., Nagamine, T., Hashimoto, N., Shibasaki, H., Takahashi, R., 2006. Generators and temporal succession of giant somatosensory evoked potentials in cortical reflex myoclonus: epicortical recording from sensorimotor cortex. Clin. Neurophysiol. 117, 1481–1486.

Huttunen, J., Kaukoranta, E., Hari, R., 1987. Cerebral magnetic responses to stimulation of tibial and sural nerves. J. Neurol. Sci. 79, 43–54.

Ikeda, A., Shibasaki, H., Nagamine, T., Xu, X., Terada, K., Mima, T., Kaji, R., Kawai, I., Tatsuoka, Y., Kimura, J., 1995. Peri-rolandic and fronto-parietal components of scalp-recorded giant SEPs in cortical myoclonus. Electroencephalogr. Clin. Neurophysiol. 96, 300–309.

Kakigi, R., Shibasaki, H., 1987a. Generator mechanisms of giant somatosensory evoked potentials in cortical reflex myoclonus. Brain 110, 1359–1373.

Kakigi, R., Shibasaki, H., 1987b. Somatosensory evoked potentials following stimulation of the lower limb in cortical reflex myoclonus. J. Neurol. Neurosurg. Psychiatry 50, 1641–1646.

Kaukoranta, E., Hari, R., Hämäläinen, M., Huttunen, J., 1986. Cerebral magnetic fields evoked by peroneal nerve stimulation. Somatosens. Res. 3, 309–321.

Lueders, H., Lesser, R.P., Hahn, J., Dinner, D.S., Klem, G., 1983. Cortical somatosensory evoked potentials in response to hand stimulation. J. Neurosurg. 58, 885–894.

Mauguiére, F., Desmedt, J.E., Courjon, J., 1983. Astereognosis and dissociated loss of frontal and parietal components of somatosensory evoked potentials in hemispheric lesions. Brain 106, 271–311.

Mima, T., Nagamine, T., Ikeda, A., Yazawa, S., Kimura, J., Shibasaki, H., 1998. Pathogenesis of cortical myoclonus studied by magnetoencephalography. Ann. Neurol. 43, 598–607.

Obeso, J.A., Rothwell, J.C., Marsden, C.D., 1985. The spectrum of cortical myoclonus. From focal reflex jerks to spontaneous motor epilepsy. Brain 108, 193–224.

Rossini, P.M., Gigli, G.L., Marciani, M.G., Zarola, F., Caramia, M., 1987. Non-invasive evaluation of input-output characteristics of sensorimotor cerebral areas in healthy humans. Electroencephalogr. Clin. Neurophysiol. 68, 88–100.

Rothwell, J.C., Obeso, J.A., Marsden, C.D., 1984. On the significance of giant somatosensory evoked potentials in cortical myoclonus. J. Neurol. Neurosurg. Psychiatry 47, 33–42.

Sendrowski, K., Sobaniec, W., Boćkowski, L., Kułak, W., Smigielska-Kuzia, J., 2010. Somatosensory evoked potentials in epileptic children treated with carbamazepine or valproate in monotherapy — a preliminary study. Adv. Med. Sci. 55, 212–215.

Shibasaki, H., Yamashita, Y., Kuroiwa, Y., 1978. Electroencephalographic studies myoclonus. Brain 101, 447–460.

Striano, P., Manganelli, F., Boccella, P., Perretti, A., Striano, S., 2005. Levetiracetam in patients with cortical myoclonus: a clinical and electrophysiological study. Mov. Disord. 20, 1610–1614.

Torquati, K., Pizzella, V., Della Penna, S., Franciotti, R., Babiloni, C., Rossini, P.M., Romani, G.L., 2002. Comparison between SI and SII responses as a function of stimulus intensity. Neuroreport 13, 813–819.

Uesaka, Y., Terao, Y., Ugawa, Y., Yumoto, M., Hanajima, R., Kanazawa, I., 1996. Magnetoencephalographic analysis of cortical myoclonic jerks. Electroencephalogr. Clin. Neurophysiol. 99, 141–148.

Uncini, A., Basciani, M., Di Muzio, A., Antonini, D., Onofrj, M., 1990. Methyl bromide myoclonus: an electrophysiological study. Acta Neurol. Scand. 81, 159–164.

Valeriani, M., Restuccia, D., Di Lazzaro, V., Le Pera, D., Tonali, P., 1997. The pathophysiology of giant SEPs in cortical myoclonus: a scalp topography and dipolar source modeling study. Electroencephalogr. Clin. Neurophysiol. 104, 122–131.